AD-A125 634 CALCULATION OF THREE-DIMENSIONAL BOUNDARY LAYERS ON BODIES AT INCIDENCE(U) IOWA INST OF HYDRAULIC RESEARCH IOWA CITY V C PATEL ET AL. SEP 82 IIHR-256 1/1

UNCLASSIFIED N00014-82-K-0200 F/G 20/4 NL

END
DATE
FILMED
4 83
DTIC

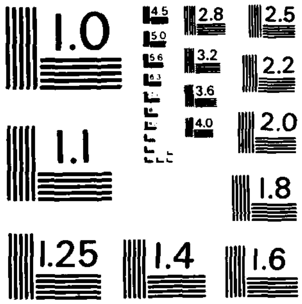

MICROCOPY RESOLUTION TEST CHART
NATIONAL BUREAU OF STANDARDS - 1963 - A

12

CALCULATION OF THREE-DIMENSIONAL BOUNDARY LAYERS ON BODIES AT INCIDENCE

by

V. C. Patel and J. H. Baek

Sponsored by
General Hydromechanics Research Program
of the Naval Sea Systems Command
Naval Ship Research and Development Center
Contract No. N00014-82-K0200

and

U.S. Army Research Office and
U.S. Air Force Office of Scientific Research
Grant No. AFOSR-80-0148-B

Based on presentation at the 7th U.S. Air Force and Federal Republic of Germany Data Exchange Agreement Meeting, "Viscous and Interacting Flow Field Effects," U.S. Army BRL, Aberdeen Proving Grounds, Md., May 26-27, 1982

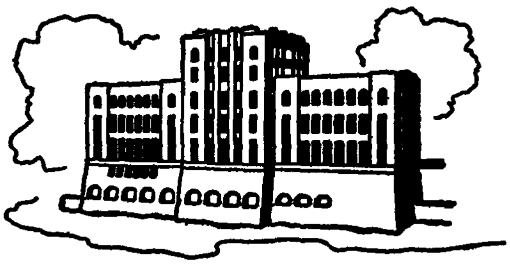

IIHR Report No. 256

Iowa Institute of Hydraulic Research
The University of Iowa
Iowa City, Iowa 52242

September 1982

Approved for public release, distribution unlimited

CALCULATION OF THREE-DIMENSIONAL BOUNDARY LAYERS ON BODIES AT INCIDENCE

by

V. C. Patel and J. H. Baek

Sponsored by
General Hydromechanics Research Program
of the Naval Sea Systems Command
Naval Ship Research and Development Center
Contract No. N00014-82-K0200

and

U.S. Army Research Office and
U.S. Air Force Office of Scientific Research
Grant No. AFOSR-80-0148-B

Based on presentation at the 7th U.S. Air Force and Federal
Republic of Germany Data Exchange Agreement Meeting, "Viscous and
Interacting Flow Field Effects," U.S. Army BRL, Aberdeen Proving Grounds,
Md., May 26-27, 1982

IIHR Report No. 256

Iowa Institute of Hydraulic Research
The University of Iowa
Iowa City, Iowa 52242

September 1982

Approved for public release, distribution unlimited

UNCLASSIFIED

SECURITY CLASSIFICATION OF THIS PAGE (When Data Entered)

REPORT DOCUMENTATION PAGE		READ INSTRUCTIONS BEFORE COMPLETING FORM
1. REPORT NUMBER	2. GOVT ACCESSION NO. AD-A125 634	3. RECIPIENT'S CATALOG NUMBER
4. TITLE (and Subtitle) Calculation of Three-Dimensional Boundary Layers on Bodies at Incidence		5. TYPE OF REPORT & PERIOD COVERED FINAL OCTOBER 80-OCTOBER 82
		6. PERFORMING ORG. REPORT NUMBER IIHR Report No. 256
7. AUTHOR(s) V.C. Patel and J.H. Baek		8. CONTRACT OR GRANT NUMBER(s) N00014-82-K0200 AFOSR-80-0148-B
9. PERFORMING ORGANIZATION NAME AND ADDRESS Iowa Institute of Hydraulic Research The University of Iowa: Iowa City, Iowa 52242		10. PROGRAM ELEMENT, PROJECT, TASK AREA & WORK UNIT NUMBERS
11. CONTROLLING OFFICE NAME AND ADDRESS DWT Naval Ship Research & Development Center Bethesda, Md 20084		12. REPORT DATE September 1982
		13. NUMBER OF PAGES 20
14. MONITORING AGENCY NAME & ADDRESS(if different from Controlling Office)		15. SECURITY CLASS. (of this report) UNCLASSIFIED
		15a. DECLASSIFICATION/DOWNGRADING SCHEDULE

16. DISTRIBUTION STATEMENT (of this Report)

Approved for Public Release; Distribution Unlimited

17. DISTRIBUTION STATEMENT (of the abstract entered in Block 20, if different from Report)

18. SUPPLEMENTARY NOTES

19. KEY WORDS (Continue on reverse side if necessary and identify by block number)

Boundary Layer; Three-Dimensional;Laminar;Turbulent;Transitional; Numerical Solutions

20. ABSTRACT (Continue on reverse side if necessary and identify by block number)

Three-dimensional thin boundary-layer equations for laminar and turbulent flows are solved by two different numerical schemes. The methods are applied to the flow over bodies of revolution at incidence and the results are compared with the available experimental data in order to study the range of validity of the classical boundary-layer approximations in regions of increasing circumferential gradients and flow reversal associated with the early stages of a free-vortex type of separation. Comparison with the DFVLR 6:1 spheroid data of Meier et al and the 4:1 comination-body data of Ramaprian, Patel and Choi

DD FORM 1 JAN 73 1473 EDITION OF 1 NOV 65 IS OBSOLETE

S/N 0102-014-6601

UNCLASSIFIED

SECURITY CLASSIFICATION OF THIS PAGE (When Data Entered)

indicate that the methods perform well in regions where the boundary layer remains thin but the predictions deteriorate as the boundary layer thickens. The results point out the need for the development of methods to handle thick boundary layers and viscous-inviscid interactions.

Accession For	
NTIS GRA&I	☑
DTIC TAB	☐
Unannounced	☐
Justification	
By	
Distribution/	
Availability Codes	
Dist	Avail and/or Special
A	

ABSTRACT

Three-dimensional thin boundary-layer equations for laminar and turbulent flows are solved by two different numerical schemes. The methods are applied to the flow over bodies of revolution at incidence and the results are compared with the available experimental data in order to study the range of validity of the classical boundary-layer approximations in regions of increasing circumferential gradients and flow reversal associated with the early stages of a free-vortex type of separation. Comparison with the DFVLR 6:1 spheroid data of Meier et al and the 4:1 combination-body data of Ramaprian, Patel and Choi indicate that the methods perform well in regions where the boundary layer remains thin but the predictions deteriorate as the boundary layer thickens. The results point out the need for the development of methods to handle thick boundary layers and viscous-inviscid interactions.

1. INTRODUCTION

The viscous flow on a body of revolution at incidence is being used as a vehicle for the development of general methods for the calculation of three-dimensional laminar and turbulent boundary layers. Although this is a simple shape, it is of considerable practical interest not only in its own right but also because it exhibits all the complex flow phenomena observed on other geometries, such as airplane fuselages and ship hulls.

The two calculation methods employed here have been described elsewhere [1,2,3] in some detail. For the present purposes it suffices to note that both solve the usual thin boundary-layer equations but differ in their numerical content and turbulence model. Thus, one of these [1] uses the Crank-Nicolson finite-difference scheme and the two-layer isotropic eddy-viscosity model of Cebeci and Smith [4]. This method was also used recently

[5] to perform calculations for four of the five test cases considered at the 1982 Eurovisc Workshop. The second method is more versatile insofar as it can accomodate flow reversal in planes normal to the marching direction. This is accomplished by the use of the ADI (Alternating-Direction-Implicit) numerical scheme. Here the turbulence model is based on the turbulent kinetic energy equation, a prescribed length-scale distribution and the assumption that the directions of the stress and rate-of-strain vectors are coincident. Both methods are capable of calculating laminar as well as turbulent boundary layers. Transition is simulated by 'switching-on' the turbulence model at prescribed positions.

This paper provides a summary of some of the calculations that have been performed to date. Since the methods have been subjected to rigorous numerical tests in laminar flows [1,3], attention will be focused on turbulent boundary layers and situations involving transition.

2. TEST CASES

Experimental data from two different bodies are now available for the assessment of the calculation methods. The model of Ramaprian, Patel and Choi [6] consisted of a hemisphere attached to a half spheroid (Fig. 1a). Transition was fixed at $X/L = 0.04$ by means of a trip wire and mean-velocity profiles were measured at several circumferential positions at each of the seven longitudinal stations. The surface pressure distribution was also recorded in some detail. Although three sets of data, corresponding to incidences $\alpha = 0$, 6 and 15 degrees, are available [6,7], we shall present calculations only for the highest incidence.

The second experiment is being conducted at the DFVLR in the Federal Republic of Germany [see, for example, 8-11] using a 2.4 m long, 6:1 prolate

spheroid (Fig. 1b). A distinctive feature of this experiment is that no tripping device is used and therefore the initially laminar boundary layer becomes turbulent through a region of natural transition. Detailed measurements of surface pressure distributions and wall shear stress have been made at two Reynolds numbers and several incidences in the range $0 < \alpha < 40^0$. However, measurements of mean-velocity profiles and Reynolds stresses are in progress for the case $\alpha = 10$ degrees at the higher Reynolds number, namely $\frac{U_\infty L}{\nu} = 7.2 \times 10^6$ ($U_\infty = 45$ m/s), where U_∞ is the reference velocity in the wind tunnel, L is the length of the body and ν is kinematic viscosity. Consequently, for the purposes of the present paper, we shall concentrate on this case although it is useful to briefly review the results of the purely laminar-flow calculations which correspond to the experiments at the lower Reynolds number.

3. CALCULATIONS

All calculations have been performed in a body-fitted (x,y,θ) coordinate system, in which x is measured from the nose along the surface, y is normal to the surface and θ is the angle measured from the windward plane of symmetry. In the presentation and discussion of the results, however, we shall refer to the distance X measured along the axis of the body. The components of mean velocity along (x,y,θ) are (U,V,W), respectively, and the components of skin-friction (wall shear) coefficient $C_f \equiv \tau_w/\frac{1}{2}\rho U_\infty^2$ along (x,θ) will be denoted by C_{fx} and C_{fz}, τ_w being the resultant wall shear stress and ρ the density.

(a) Laminar Flow

Laminar boundary layer calculations were performed, by both the Crank-Nicolson (CN) and the ADI methods, for the DFVLR spheroid at $\alpha = 10^0$, assuming

inviscid-flow pressure distribution, and starting at the forward stagnation point. As discussed in [3], the CN method is able to calculate the boundary layer only in the region between the windward plane and a line on the body along which the circumferential component of velocity changes sign (from positive to negative) or, equivalently, C_{fz} vanishes. This method can, however, be used to perform a separate calculation along the leeward plane of symmetry. The ADI method, on the other hand, continues to provide a solution on both sides of this circumferential flow-reversal (CFR) line.

Figure 2 shows a comparison between the CFR line indicated by the DFVLR measurements of wall shear stress at the lower Reynolds number of 1.6 x 10^6 (U_∞ = 10 m/s) and those predicted by the two methods. It is seen that the results of the two methods agree quite well with each other and both predictions are in excellent agreement with experiment.

The circumferential distributions of the components of wall shear stress at three representative axial stations, as determined by the ADI method, are compared with the corresponding experimental results in Fig. 3. The disagreement between the data and these laminar calculations at $\theta = 150^\circ$, X/L = 0.381 and in $120^\circ < \theta < 165^\circ$, X/L = 0.64, is due to a growing wedge of turbulent flow on the leeside beyond the CFR line. The circumferential distributions of the physical boundary-layer thickness, δ, and the displacement thickness, δ^*, shown in Fig. 4 for X/L = 0.64 indicate the thickening of the boundary layer in the vicinity of the CFR line.

A particularly noteworthy feature of the ADI solutions is illustrated in Fig. 5 where several axial and circumferential velocity profiles at X/L = 0.508 are plotted in the neighborhood of the CFR line which is located at $\theta \approx 110^\circ$. The results show the rapid circumferential thickening of the boundary layer and the development of a two-layer structure. These features

are associated with the convergence of streamlines near the wall into the CFR line from both sides while the flow in the outer part continues to go from the windward to the leeward side as required by the external inviscid flow. Whether the solutions in this region can be regarded as physically realistic may be questioned since one may doubt the continued validity of the boundary-layer approximations and, as mentioned earlier, the experiments indicate transition to turbulent flow. Nevertheless, these are solutions of the first-order equations and need to be analyzed in detail in order to determine what additional terms in the equations should be retained and how to couple such a viscous flow with the external inviscid flow to develop a more general solution procedure.

(b) Turbulent Flow

For the combination body tested at Iowa [6], calculations were performed for the case of $\alpha = 15^{0}$ using the measured pressure distribution. The experiments indicated a substantial difference between the actual and the inviscid-flow pressure distributions due to viscous-inviscid interaction and therefore the use of the former represents a better test of the boundary-layer calculation methods.

The calculations were started at station 1 (X/L = 0.176) with the measured mean-velocity components. The CN method was also used to separately calculate the boundary-layer development along the leeward plane of symmetry which is not accessible to the three-dimensional calculations beyond the CFR line.

An overview of the results is provided by Figs. 6-8. In general, the agreement between the calculations and experiment is quite good on the windward side but quantitative differences arise on the leeward side, beyond

the CFR line, where the boundary layer is rather thick and the viscous-inviscid interaction is strong. The growing disagreement between the calculations and experiment on the leeward side may be attributed to the thick boundary-layer effects rather than a gross inadequacy of the turbulence models. Detailed measurements of the Reynolds stresses are required to verify this.

(c) Laminar and Turbulent Flow

The experimentally determined line of transition in the higher Reynolds number tests on the DFVLR spheroid at $\alpha = 10^{0}$ is shown in Fig. 9. This line demarcates the most upstream positions at which the wall shear stress reaches a minimum value in the local circumferential direction.

The measured pressure distributions in this case agreed quite well with potential flow over most of the body but systematic departures were noted in a region surrounding the CFR line on the leeward side. Although calculations have been performed with the measured as well as the potential-flow pressure distributions to study the influence of viscous-inviscid interaction, for the purposes of the present paper, we shall present only the solutions obtained with the potential-flow pressure distribution.

The boundary-layer calculations were started at the forward stagnation point in both the ADI and the CN methods. In both cases, the turbulence model was activated at the aforementioned transition line as it was crossed at each value of θ. Thus, in the region $0.22 < X/L < 0.56$ the boundary- layer calculations involve laminar, transitional and turbulent flow in the circumferential direction. The intermittency function in the Cebeci-Smith eddy-viscosity model used in the CN method is the same as that employed in two-dimensional flow to mimic transitional flow over a finite streamwise

distance. However, in the turbulent-kinetic-energy equation used in the ADI method, no attempt has been made to tailor the model constants or functions to optimize agreement with data even in two-dimensional flows. This difference should be taken into consideration in the discussion and interpretation of the subsequent results.

Fig. 9 shows a short CFR line in the laminar flow ahead of transition on the leeside. This is essentially the same as that calculated at the lower Reynolds number. It disappears after transition but a new CFR line is predicted in the turbulent flow further downstream. This line is of course closer to the leeside than the corresponding line in purely laminar flow, indicating the greater capability of turbulent flow to overcome the adverse circumferential pressure gradient before flow reversal. The experimentally observed CFR lines are again in good agreement with the calculations.

Detailed comparisons between the calculations and measurements are presented in Figs. 10 and 11. The former shows the variation of the two components of skin friction along a few representative generators while the latter compares the calculated velocity profiles with those measured at X/L = 0.64. It is evident from Fig. 10 that the skin-friction coefficients predicted by the two methods in the region of laminar flow are in good agreement with each other and with the experimental values. The solutions through the transition regions give remarkably good representation of the data despite the rather crude manner in which transition is simulated. In the turbulent flow, the agreement between the data and the results of both methods is again good although the experiments indicate generally higher stresses. The velocity profiles shown in Fig. 11 substantiate the observations made on the basis of wall shear stress distributions. In particular, it is seen that the predictions are in good agreement with the data over the windward side

except at $\theta = 0^0$, but systematic departures occur in the neighborhood of the CFR line ($\theta \sim 140^0$ at $X/L = 0.64$). The disagreement in the profile at $\theta = 0^0$ is due to the fact that the experimental flow is not fully turbulent at this station.

4. CONCLUSIONS

From the variety of results presented here it is apparent that three-dimensional boundary-layer calculation methods considered here have reached a stage where they can be used with confidence on practical geometries provided the boundary layer remains thin and the first-order equations remain valid. Laminar and turbulent-flow calculations in regions of circumferential-flow reversal, which are accompanied by increasing boundary-layer thickness, large circumferential gradients and strong viscous-inviscid interaction, indicate special features which need further study especially to develop practical methods for the prediction of thick boundary layers and to couple such methods to the external flow to account for viscous-inviscid interactions.

ACKNOWLEDGEMENTS

The research on the development of general calculation methods for three-dimensional boundary layers has been supported by the U.S. Army Research Office and the U.S. Air Force Office of Scientific Research under grant AFOSR-80-0148-B, and by the General Hydromechanics Research Program of the Naval Sea Systems Command of the U.S. Navy, administered by the David W. Taylor Naval Ship Research and Development Center, under Contract N00014-82-K0200.

The authors also acknowledge the timely assistance of Dr. A.W. Fiore of the AFFDL and Dr. H.U. Meier of the DFVLR, Project Officers of the Data Exchange Agreement, in making available tabulated data from the DFVLR experiments.

REFERENCES

[1] Chang, K.C. and Patel, V.C. (1975) "Calculation of Three-Dimensional Boundary Layers on Ship Forms", IIHR Report No. 178, The University of Iowa.

[2] Choi, D.H. (1978) "Three-Dimensional Boundary Layers on Bodies of Revolution at Incidence", Ph.D. Dissertation, The University of Iowa.

[3] Patel, V.C. and Choi, D.H. (1980) "Calculation of Three-Dimensional Laminar and Turbulent Boundary Layers on Bodies of Revolution at Incidence", Turbulent Shear Flow 2, Springer-Verlag, pp. 199-217.

[4] Cebeci, T. and Smith, A.M.O. (1974) "Analysis of Turbulent Boundary Layers", Academic Press.

[5] Patel, V.C., Krogstad, P.A. and Baek, J.H. (1982) "Three-Dimensional Turbulent Boundary-Layer Calculations by an Implicit Crank-Nicolson Method", EUROVISC Workshop on 3D Boundary Layers, Berlin, Apr. 1, 1982. Also, Iowa Institute of Hydraulic Research, IIHR Report No. 254.

[6] Ramaprian, B.R., Patel, V.C., and Choi, D.H. (1981) "Mean-Flow Measurements in the Three-Dimensional Boundary Layer Over a Body of Revolution at Incidence", J. Fluid Mech., Vol. 103, pp. 479-504.

[7] Ramaprian, B.R. and Novak, C.J. (1980) "Mean Flow Measurements in the Three-Dimensional Boundary Layer Over a Body of Revolution at Incidence: Part II", IIHR Limited Distribution Report 76, The University of Iowa.

[8] Meier, H.U., Kreplin, H.P. and Vollmers, H. (1981) "Velocity Distributions in 3-D Boundary Layers and Vortex Flows on an Inclined Prolate Spheroid", Proc. 6th USAF-FRG Data Exchange Agreement Meeting, Gottingen, DFVLR-AVA Report IB 22281 CP1, pp. 202-217.

[9] Meier, H.U. and Kreplin, H.P. (1980) "Experimental Study of Boundary Layer Velocity Profiles on a Prolate Spheroid at Low Incidence in the Cross-Section x/L = 0.64", Proc. 5th USAF-FRG DEA Meeting, AFFDL-TR-80-3088, pp. 169-189.

[10] Meier, H.U., and Kreplin, H.P. (1980) "Experimental Investigations of Boundary Layer Transition and Separation on a Body of Revolution", Z. Flugwiss Weltraumforschung, Vol. 4, pp. 65-71.

[11] Kreplin, H.P., Meier, H.U., and Maier, A. (1978) "Wind Tunnel Model and Measuring Techniques for the Investigatiion of Three-Dimensional Boundary Layers", AIAA Paper 78-781.

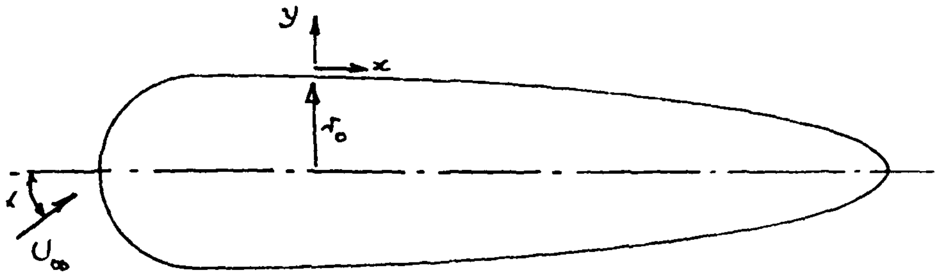

(a) Combination body [6]

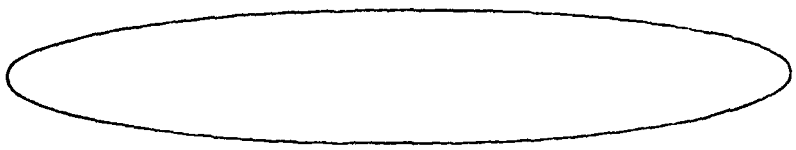

(b) Spheroid [8]

Fig. 1. Shapes of models tested

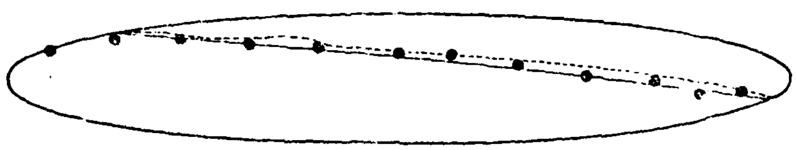

Fig. 2. Circumferential flow reversal line: spheroid, laminar flow. ● Expt, —— ADI, ----- CN.

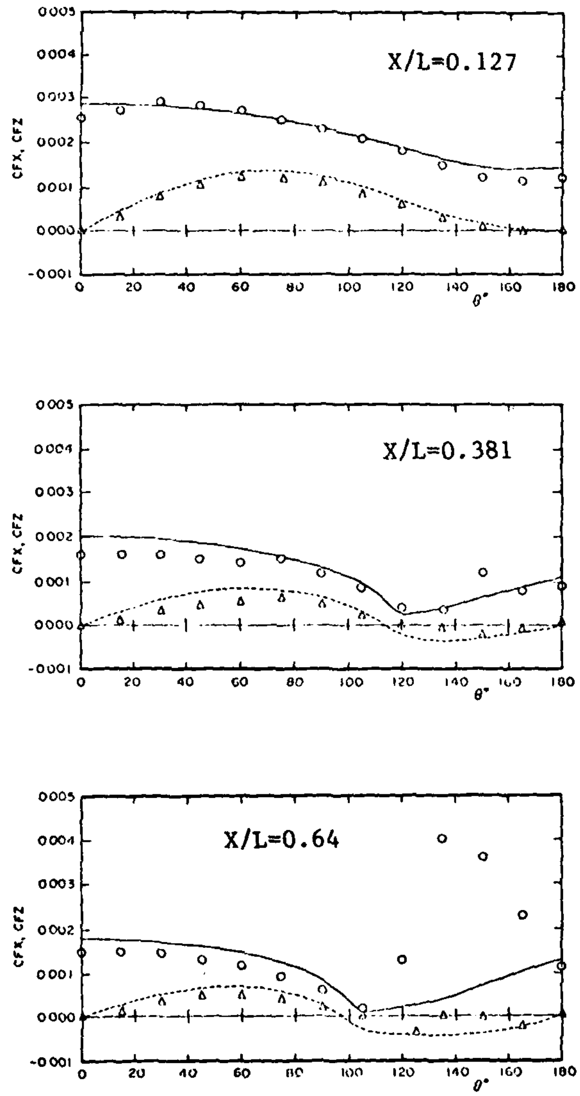

Fig.3. Circumferential variation of C_{fx},$C_{f\theta}$ on spheroid, α=10 Deg. Laminar flow

Lines:ADI solution, Symbols:DFVLR data

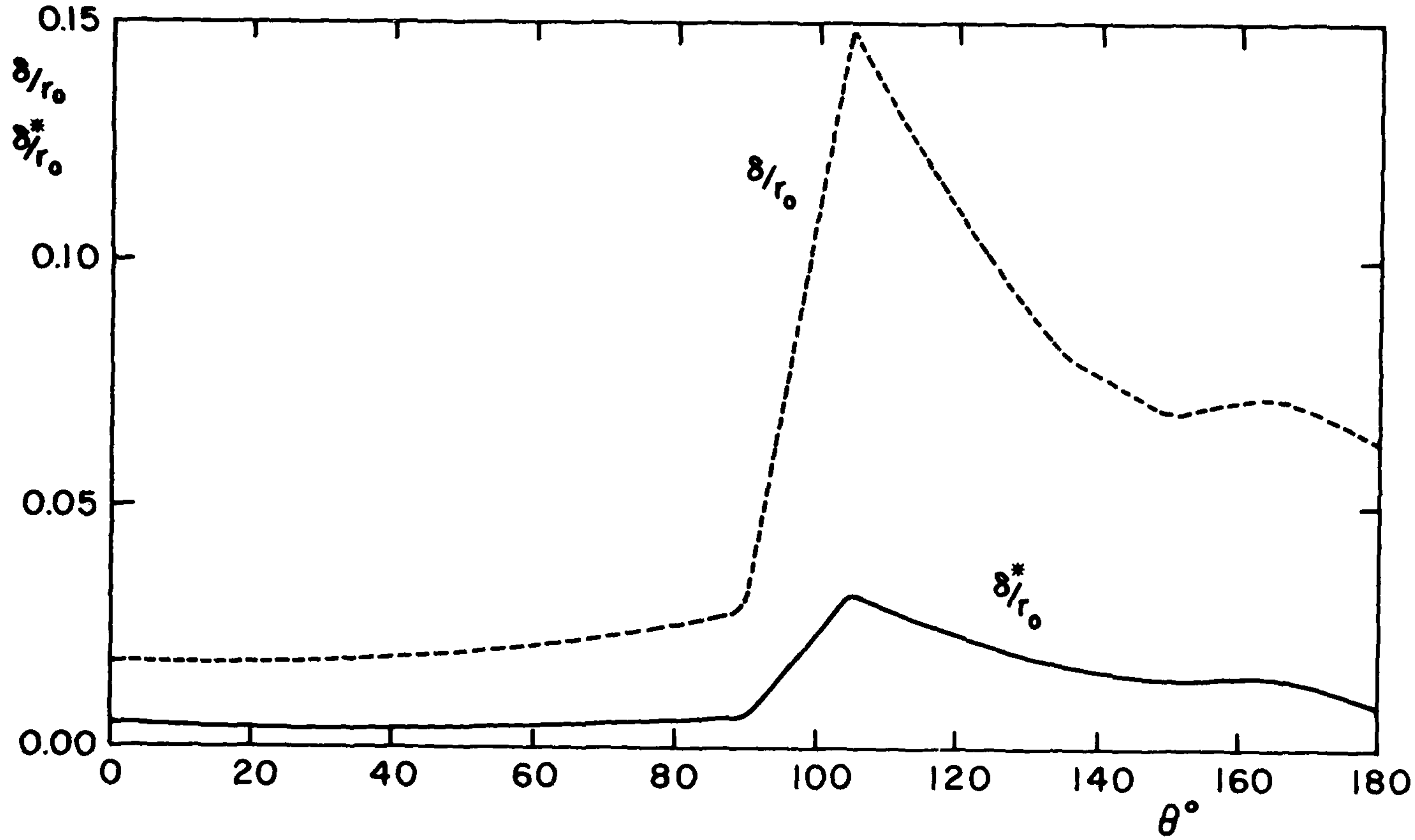

Fig. 4. Spheroid, laminar flow. Boundary layer thicknesses at $X/L = 0.64$.

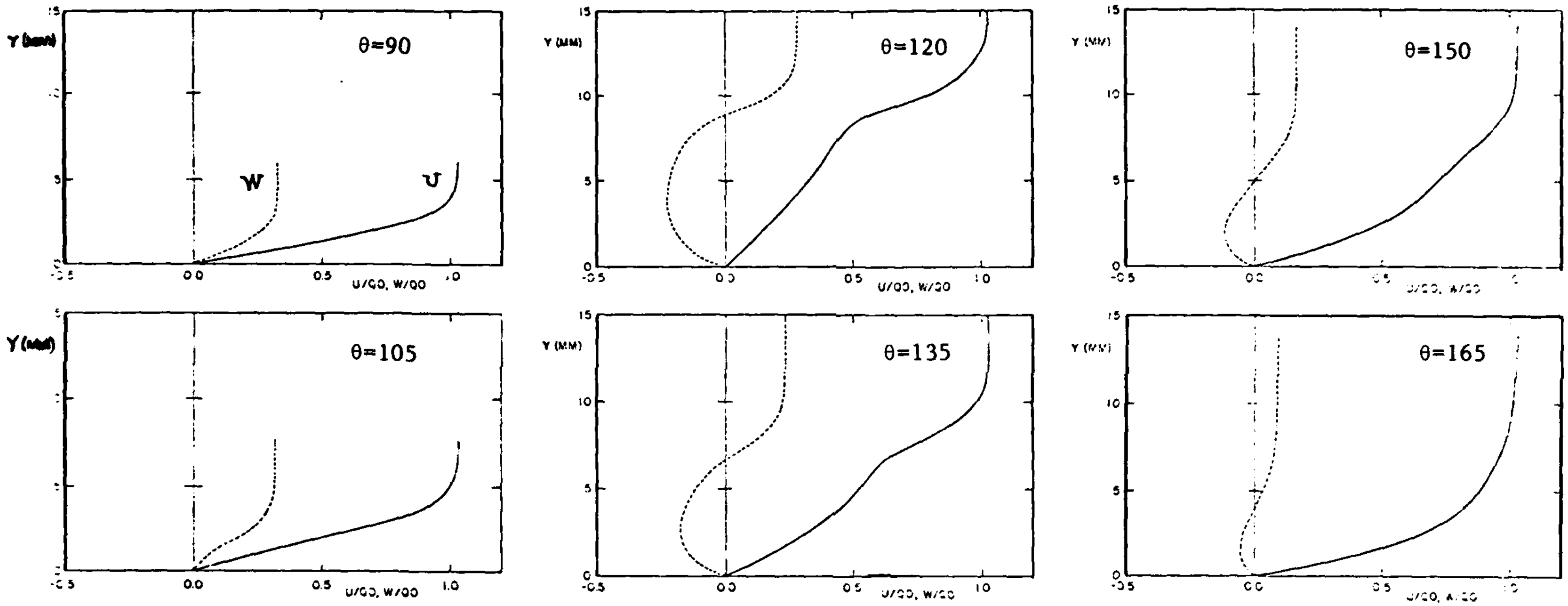

Fig.5. Velocity profiles in laminar boundary layer on spheroid, α=10 Deg. X/L=0.508

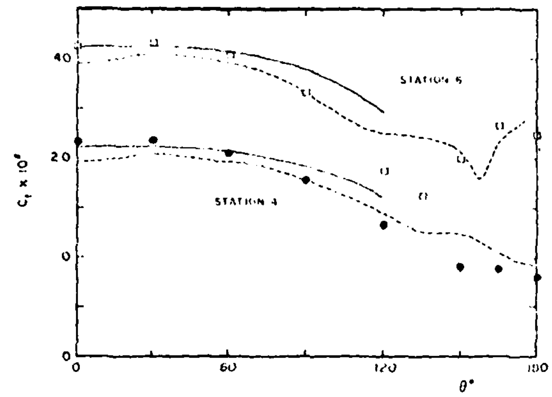

Fig.6. Circumferential variations of C_f on combination body, α=15 Deg. Turbulent flow ; —— CN, ---- ADI

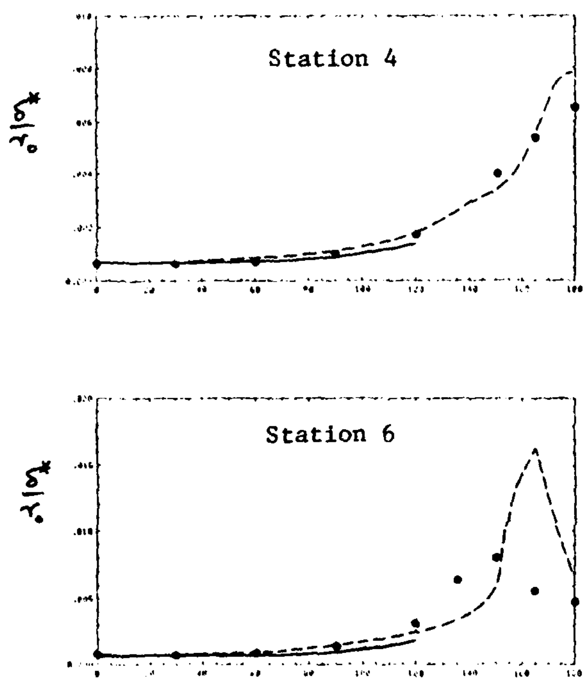

Fig.7. Circumferential variations of δ^* on combination body, α=15 Deg. Turbulent flow ; —— CN, ---- ADI

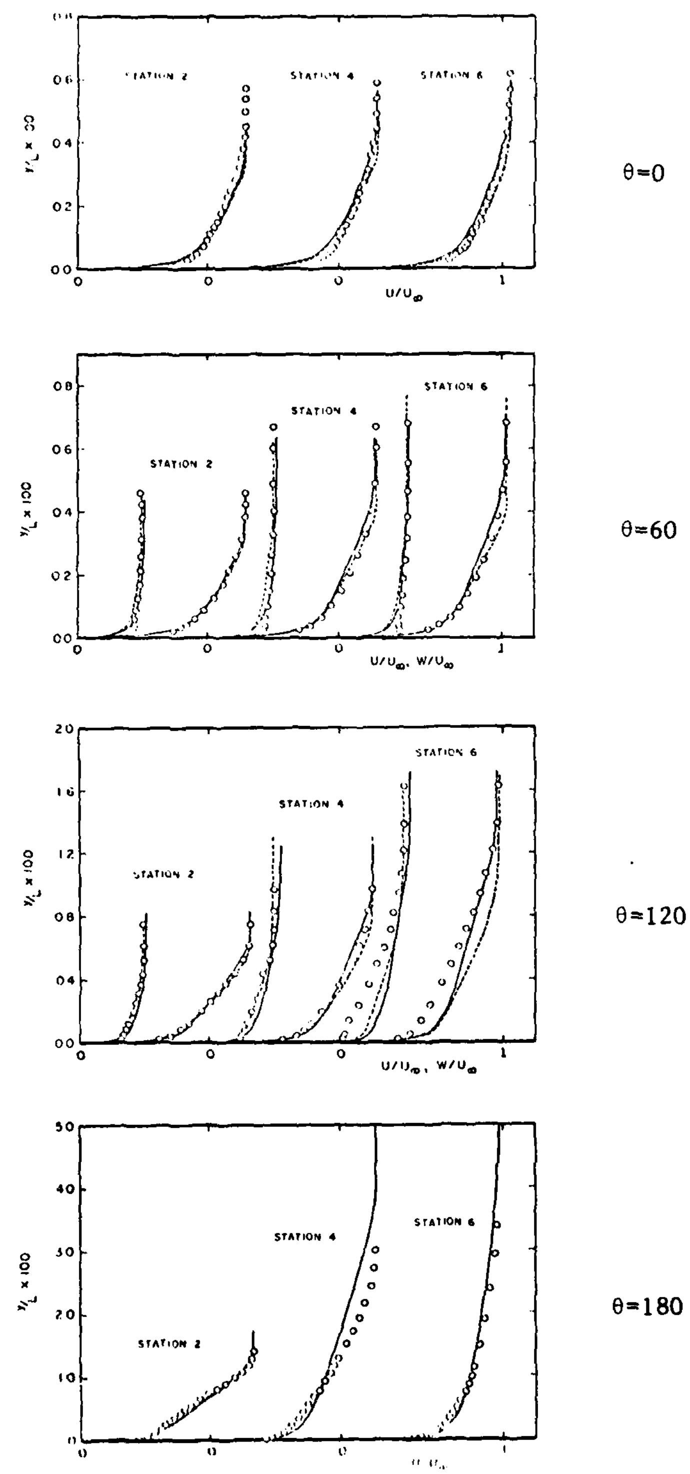

Fig.8. Velocity profiles on combination body,
α=15 Deg. Turbulent flow ; --- CN, —— ADI

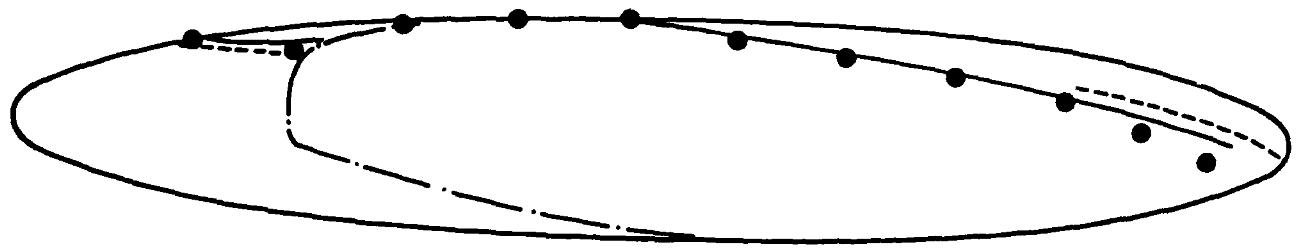

Fig. 9. Circumferential flow reversal line: spheroid, laminar and turbulent flow. ● Expt., —— ADI, ----- CN; —·— Experimental transition line.

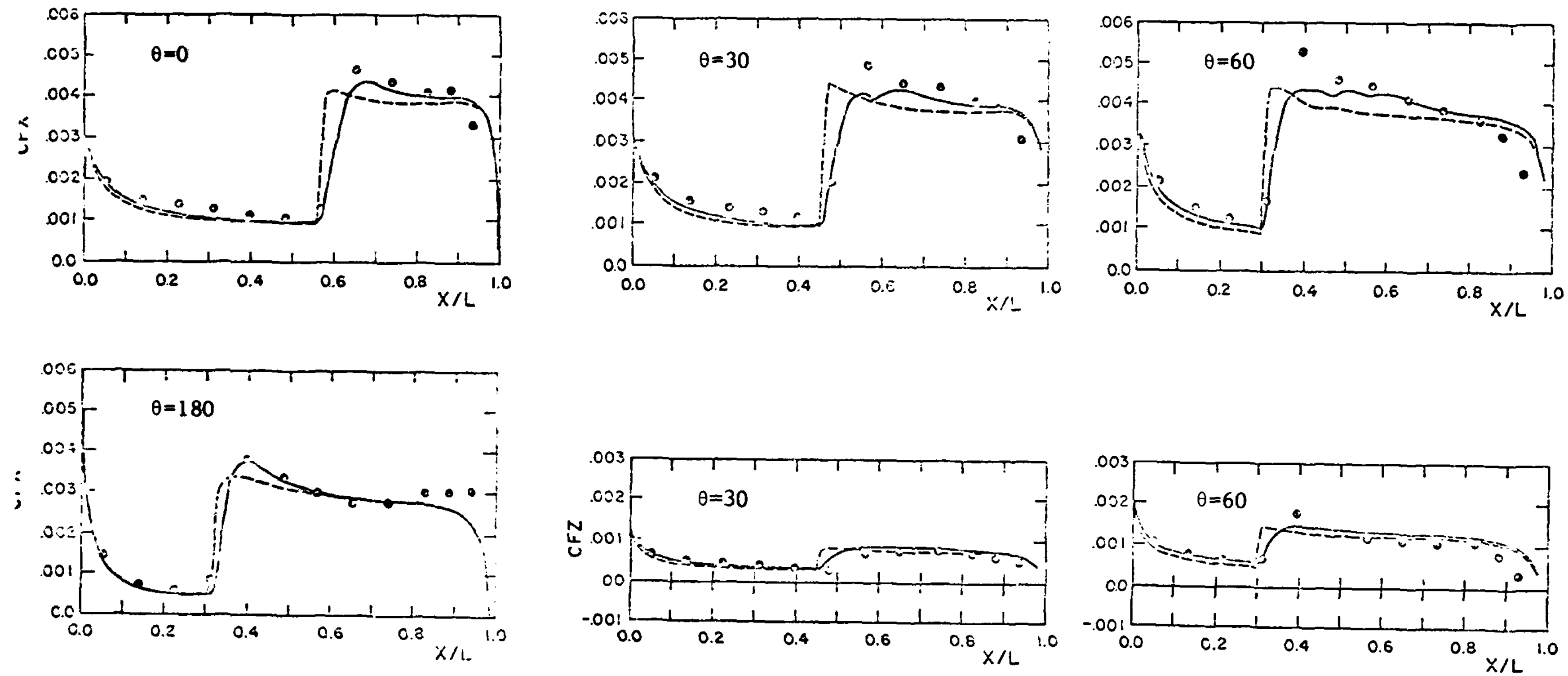

Fig.10. Axial variations of C_{fx} and $C_{f\theta}$ on spheroid,
α=10 Deg. Transitional flow
---- ADI , —— CN , Symbols:Experiment

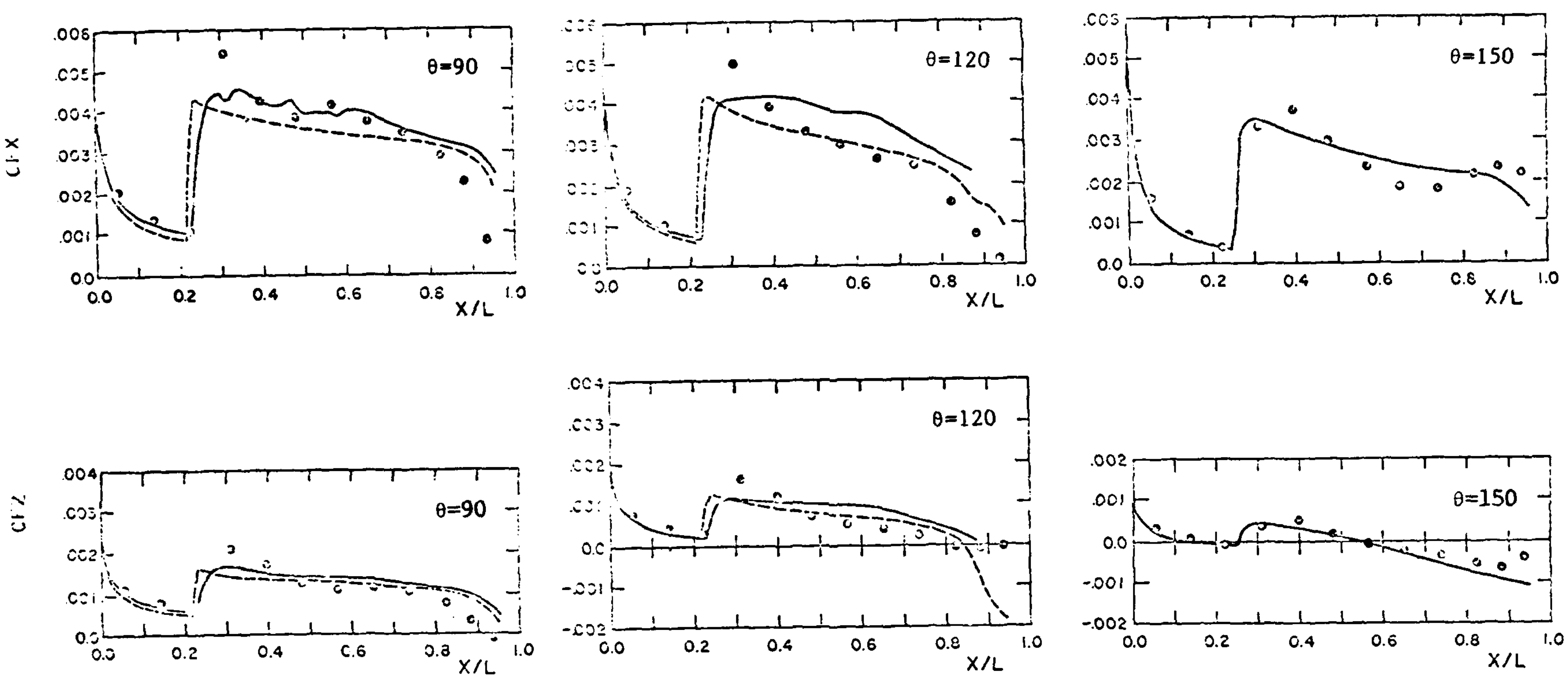

Fig.10. Continued

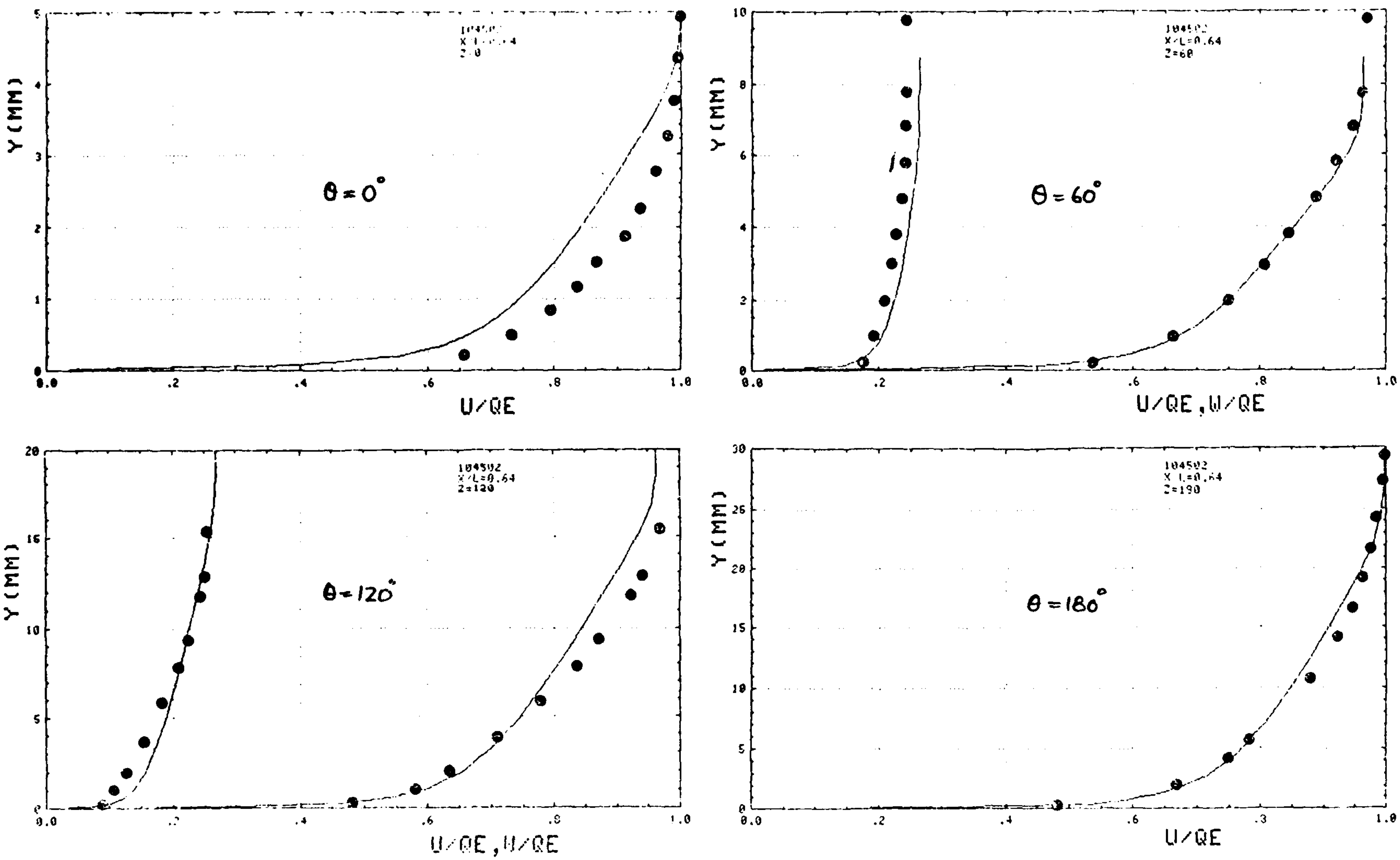

Fig.11. Profiles of axial and circumferential components of velocity at X/L=0.64 on spheroid, α=10 Deg. Transitional flow ; —— ADI , ● Experiment

DISTRIBUTION LIST FOR REPORTS PREPARED UNDER THE GENERAL HYDROMECHANICS RESEARCH PROGRAM

Commander
David W. Taylor Naval Ship
R & D Center (ATTN: Code 1505)
Bldg. 19, Room 129B
Bethesda, Maryland 20084
15 Copies

Commander
Naval Sea Systems Command
Washington, D.C. 20362
ATTN: 05R22 (J. Sejd)

Commander
Naval Sea Systems Command
Washington, D.C. 20362
ATTN:55W (R. Keane, Jr.)

Commander
Naval Sea Systems Command
Washington, D.C. 20362
ATTN: 55W3 (W. Sandberg)

Commander
Naval Sea Systems Command
Washington, D.C. 20362
ATTN: 50151 (C. Kennell)

Commander
Naval Sea Systems Command
Washington, D.C. 20362
ATTN: 56X1 (F. Welling)

Commander
Naval Sea Systems Command
Washington, D.C. 20362
ATTN: 63R31 (T. Pierce)

Commander
Naval Sea Systems Command
Washington, D.C. 20362
ATTN: 55X42 (A. Paladino)

Commander
Naval Sea Systems Command
Washington, D.C. 20362
ATTN: 99612 (Library)

Director
Defense Documentation Center
5010 Duke Street
Alexandria, Va 22314
12 copies

Library of Congress
Science & Technology Division
Washington, D.C. 20540

Naval Ship Engineering Center
Norfolk Division
Combatant Craft Engr Dept
Attn: D. Blount (6660)
Norfolk, VA 23511

Naval Underwater Weapons Research
& Engineering Station (Library)
Newport, R.I. 02840

Office of Naval Research
800 N. Quincy Street
Arlington, Virginia 22217
ATTN: Dr. C.M. Lee, Code 432

Commanding Officer (L31)
Naval Civil Engineering Laboratory
Port Hueneme, CA 93043

Commander
Naval Ocean Systems Center
San Diego, CA 92152
Attn: Library

Library
Naval Underwater Systems Center
Newport, RI 02840

Research Center Library
Waterways Experiment Station
Corps of Engineers
P.O. Box 631
Vicksburg, Mississippi 39180

Charleston Naval Shipyard
Technical Library
Naval Base
Charleston, S.C. 29408

Norfolk Naval Shipyard
Technical Library
Portsmoth, VA 23709

Puget Sound Naval Shipyard
Engineering Library
Bremerton, WA 98314

Long Beach Naval Shipyard
Technical Library (246L)
Long Beach, CA 90801

Mare Island Naval Shipyard
Shipyard Technical Library (202.3)
Vallejo, CA 94592

Assistant Chief Design Engineer
for Naval Architecture (Code 250)
Mare Island Naval Shipyward
Vallejo, CA 94592

U.S. Naval Academy
Annapolis, Md 21402
Attn: Technical Library

Naval Postgraduate School
Monterey, CA 93940
Attn: Library (2124)

Study Center
National Maritime Research Center
U.S. Merchant Marine Academy
Kings Point, LI, New York 11024

The Pennsylvania State University
Applied Research Laboratory (Library)
P.O. Box 30
State College, PA 16801

Dr. B. Parkin, Director
Garfield Thomas Water Tunnel
Appliled Research Laboratory
P.O. Box 30
State College, PA

Bolt, Beranek & Newman (Library)
50 Moulton Street
Cambridge, MA 02138

Bethlehem Steel Corporation
25 Broadway
New York, New York 10004
Attn: Library-Shipbuilding

Cambridge Acoustical Associates, Inc.
54 Rindge Ave Extension
Cambridge, MA 02140

R & D Manager
Electric Boat Division
General Dynamics Corporation
Groton, Conn 06340

Gibbs & Cox, Inc. (Tech Info Control)
21 West Street
New York, New York 10006

Hydronautics, Inc. (Library)
Pindell School Rd.
Laurel, MD 20810

Newport News Shipbuilding and Dry
Dock Company (Tech. Library)
4101 Washington Ave.
Newport News, VA 23607

Mr. S. Spangler
Nielsen Engineering & Research, Inc.
510 Clyde Ave.
Mountain View, CA 94043

Society of Naval Architects and
Marine Engineers (Tech Library)
One World Trade Center, Suite 1369
New York, NY 10048

Sun Shipbuilding & Dry Dock Co.
Attn: Chief Naval A rchitect
Chester, PA 19000

Sperry Systems Management Division
Sperry Rand Corporation (Library)
Great Neck, N.Y. 10020

Stanford Research Institute
Attn: Library
Menlo Park, CA 94025

Southwest Research Institute
P.O. Drawer 28510
San Antonio, TX 78284
Attn: Applied Mech. Review
Dr. H. Abramson
2 copies

Tracor, Inc.
6500 Tracor Lane
Austin, Texas 78721

Mr. Robert Taggart
9411 Lee Highway, Suite P
Fairfax, VA 22031

Ocean Engr Department
Woods Hole Oceanographic Inc.
Woods Hole, Mass. 02543

Worcester Polytechnic Inst.
Alden Research Lab (Tech Library)
Worcester, MA 01609

Applied Physics Laboratory
University of Washington (Tech Library)
1013 N. E. 40th Street
Seattle, Washington 98105

University of California
Naval Architecture Department
Berkeley, CA 94720
4 Copies - ATTN: Profs. Webster, Paulling, Wehausen & Library

California Institute of Technology
ATTN: Library
Pasadena, CA 91109

Engineering Research Center
Reading Room
Colorado State University
Foothills Campus
Fort Collins, Colorado 80521

Florida Atlantic University
Ocean Engineering Department
Boca Raton, Florida 33432
Attn: Technical Library

Gordon McKay Library
Harvard University
Pierce Hall
Cambridge, MA 02138

Department of Ocean Engineering
University of Hawaii (Library)
2565 The Mall
Honolulu, Hawaii 96822

Institute of Hydraulic Research
The University of Iowa
Iowa City, Iowa 52242
3 copies ATTN: Library, Landweber, Patel

Prof. O. Phillips
Mechanics Department
The John Hopkins University
Baltimore, Maryland 21218

Kansas State University
Engineering Experiment Station
Seaton Hall
Manhattan, Kansas 66502

University of Kansas
Chairman, Civil Engr Department Library
Lawrence, Kansas 60644

Fritz Engr Laboratory Library
Department of Civil Engr
Lehigh University
Bethelehem, PA 18015

Department of Ocean Engineering
Massachusetts Institute of Technology
Cambridge, MA 02139
2 Copies: Attn: Profs. Leehey & Kerwin

Engineering Technical Reports
Room 10-500
Massachusetts Institute of Technology
Cambridge, MA 02139

St. Anthony Falls Hydraulic Laboratory
University of Minnesota
Mississippi River at 3rd Ave., S.E.
Minneapolis, Minnesota 55414
2 Copies: Attn: Dr. Austin & Library

Department of Naval Architecture
and Marine Engineering - North Campus
ATTN: Library
University of Michigan
Ann Arbor, Michigan 48109

Davidson Laboratory
Stevens Institute of Technology
711 Hudson Street
Hoboken, New Jersey 07030
Attn: Library

Applied Research Laboratory
University of Texas
P.O. Box 8029
Austin, Texas 78712

Stanford University
Stanford, California 94305
2 Copies:
Attn: Engineering Library, Dr. Street

Webb Institute of Naval Architecture
Attn: Library
Crescent Beach Road
Glen Cove, L.I., New York 11542

National Science Foundation
Engineering Division Library
1800 G Street N.W.
Washington, D.C. 20550

Mr. John L. Hess
4338 Vista Street
Long Beach, CA 90803

Dr. Tuncer Cebeci
Mechanical Engineering Dept.
California State University
Long Beach, CA 90840

Science Applications, Inc.
134 Holiday Court, Suite 318
Annapolis, MD 21401

END

DATE
FILMED

4-83

DTIC